Molecular exchange-correlation Kohn-Sham potential and energy density from ab initio first- and second-order density matrices: examples for XH (X=Li, B,F).

Gritsenko, O.V.; van Leeuwen, R.; Baerends, E.J.

published in
Journal of Chemical Physics
1996

DOI (link to publisher)
10.1063/1.471602

document version
Publisher's PDF, also known as Version of record

Molecular exchange-correlation Kohn–Sham potential and energy density from *ab initio* first- and second-order density matrices: Examples for XH (X=Li, B, F)

Oleg V. Gritsenko, Robert van Leeuwen, and Evert Jan Baerends
Afdeling Theoretische Chemie, Vrije Universiteit, De Boelelaan 1083, 1081 HV, Amsterdam, The Netherlands

(Received 25 January 1996; accepted 1 March 1996)

The molecular Kohn–Sham exchange-correlation potential $v_{\rm xc}$ and the energy density $\epsilon_{\rm xc}$ have been constructed from *ab initio* first- and second-order density matrices for the series XH (X=Li, B, F). The way various effects of electronic structure and electron correlation manifest themselves in the shape of $v_{\rm xc}$ and $\epsilon_{\rm xc}$ has been analyzed by their decomposition into various components; the potential of the exchange-correlation hole, the kinetic component and (in the case of $v_{\rm xc}$) the ''response'' component. The kinetic energy of noninteracting particles T_s, the kinetic part of the exchange-correlation energy T_c, and the energy of the highest occupied molecular orbital ϵ_N have been obtained with reasonable accuracy and the effect of bond formation on these functionals has been studied.[1] © *1996 American Institute of Physics.* [S0021-9606(96)03021-8]

I. INTRODUCTION

Key ingredients of the density functional theory (DFT) (Refs. 1, 2) are the exchange-correlation energy functional $E_{\rm xc}[\rho]$ of a many-electron system,

$$E_{\rm xc}[\rho]=\int \rho(\mathbf{r})\,\epsilon_{\rm xc}([\rho];\mathbf{r})\,d\mathbf{r}, \tag{1}$$

and the corresponding exchange-correlation Kohn–Sham (KS) potential $v_{\rm xc}([\rho];\mathbf{r})$,

$$v_{\rm xc}([\rho];\mathbf{r})=\frac{\delta E_{\rm xc}[\rho]}{\delta\rho(\mathbf{r})}, \tag{2}$$

the latter represents the local effect of electron exchange and Coulomb correlation in the one-electron KS equations (Hartree atomic units will be used throughout the paper)

$$\{-\tfrac{1}{2}\nabla^2+v_{\rm ext}(\mathbf{r})+v_H(\mathbf{r})+v_{\rm xc}(\mathbf{r})\}\phi_i(\mathbf{r})=\epsilon_i\phi_i(\mathbf{r}), \tag{3}$$

$$\sum_{i=1}^{N}|\phi_i(\mathbf{r})|^2=\rho(\mathbf{r}). \tag{4}$$

$E_{\rm xc}[\rho]$ is expressed in Eq. (1) as an integral of the exchange-correlation energy density per particle $\epsilon_{\rm xc}([\rho];\mathbf{r})$, while $v_{\rm xc}([\rho];\mathbf{r})$ is defined in Eq. (2) as a functional derivative of $E_{\rm xc}[\rho]$ with respect to the electron density $\rho(\mathbf{r})$. In Eq. (3) $v_{\rm ext}$ is the external potential, v_H is the Hartree potential of the electrostatic electron repulsion, N is the number of electrons in the system, and the occupied KS orbitals ϕ_i yield ρ via Eq. (4).

The exact functional form of $v_{\rm xc}$ and $\epsilon_{\rm xc}$ is not known. However, several methods have been proposed[3–10] to construct $v_{\rm xc}$ numerically using an essentially accurate ρ from *ab initio* calculations. Hitherto, all these methods have been applied to few-electron atomic systems and only recently the first example of a v_{xc} has been obtained with the method of Ref. 9 for a molecular system with $N>2$, namely, the LiH molecule.[11]

For the analysis of electron interaction and for efficient DFT approximation of $v_{\rm xc}$ it is useful to decompose $v_{\rm xc}$ into various components related to the electronic structure. In particular, one can decompose $v_{\rm xc}$ into the ''energy'' and ''response'' components.[12] The former, namely, the potential of the exchange-correlation hole $v_{\rm xc}^{\rm hole}$ and the potential $v_{c,\rm kin}$, representing the effect of Coulomb correlation on the kinetic functional, contribute also to the exchange-correlation energy functional. The latter represent ''response'' effects on $v_{\rm xc}^{\rm hole}$ and $v_{c,\rm kin}$ and do not contribute to $E_{\rm xc}[\rho]$. Such a decomposition has been carried out[12] for the atomic exchange-only potentials of the optimized potential model (OPM) (Refs. 13–15) and also for $v_{\rm xc}$ of the two-electron He atom and H_2 molecule.[16] However, to our best knowledge, $v_{\rm xc}$ for systems with $N>2$ have never been analyzed in this way.

Unlike $v_{\rm xc}$, which is defined uniquely (up to a constant) for a given system with Eq. (2), $\epsilon_{\rm xc}$ is not defined uniquely with Eq. (1), since the same $E_{\rm xc}$ can be obtained with different functions $\epsilon_{\rm xc}(\mathbf{r})$ and $\epsilon'_{\rm xc}(\mathbf{r})=\epsilon_{\rm xc}(\mathbf{r})+f(\mathbf{r})$ whose difference $f(\mathbf{r})$ integrates to zero

$$\int \rho(\mathbf{r})f(\mathbf{r})\,d\mathbf{r}=0. \tag{5}$$

Nevertheless, in order to perform a consistent analysis of correlation effects and to provide a physically reasonable modeling of $\epsilon_{\rm xc}$ one can choose some suitable definition of $\epsilon_{\rm xc}(\mathbf{r})$. In particular, one can express $\epsilon_{\rm xc}$ as a combination of $v_{\rm xc}^{\rm hole}$ and $v_{c,\rm kin}$ (Ref. 17). (See also the next section for this definition.) A procedure to construct $\epsilon_{\rm xc}$ from *ab initio* first- and second-order density matrices has been proposed in Ref. 17 and examples of the correlation energy density ϵ_c have been obtained for the two-electron systems He and H_2.

This paper presents molecular v_{xc} and ϵ_{xc} constructed from *ab initio* first- and second-order density matrices for the closed-shell monohydrides of elements of the second period LiH, BH, and HF. The corresponding KS energy characteristics such as the kinetic energy of noninteracting particles T_s, the kinetic part of the correlation energy T_c and the energy of the highest occupied molecular orbital (HOMO) ϵ_N are also calculated and discussed. The relation between the form of v_{xc} and the molecular electronic structure is analyzed via the decomposition of v_{xc} into v_{xc}^{hole}, $v_{c,kin}$ and the response potential.

II. PARTITIONING OF v_{xc} AND ϵ_{xc}

To define ϵ_{xc} and to provide a partitioning for v_{xc}, we use the following expression for $E_{xc}[\rho]$;[12,17]

$$E_{xc}[\rho]=W_{xc}[\rho]+T_c[\rho], \tag{6}$$

$$W_{xc}[\rho]=\frac{1}{2}\int \rho(\mathbf{r})v_{xc}^{hole}(\mathbf{r})d\mathbf{r}, \tag{7}$$

$$T_c[\rho]=\int \rho(\mathbf{r})[v_{kin}(\mathbf{r})-v_{s,kin}(\mathbf{r})]d\mathbf{r}. \tag{8}$$

The first term of Eq. (6) is the potential (i.e., electron–electron interaction) contribution W_{xc} to E_{xc} with v_{xc}^{hole} in Eq. (7) being the potential of the exchange-correlation hole,

$$v_{xc}^{hole}(\mathbf{r}_1)=\int \frac{\rho_2(\mathbf{r}_1,\mathbf{r}_2)-\rho(\mathbf{r}_1)\rho(\mathbf{r}_2)}{|\mathbf{r}_1-\mathbf{r}_2|\rho(\mathbf{r}_1)}\,d\mathbf{r}_2 = \int \frac{\rho(\mathbf{r}_2)[g(\mathbf{r}_1,\mathbf{r}_2)-1]}{|\mathbf{r}_1-\mathbf{r}_2|}\,d\mathbf{r}_2. \tag{9}$$

In Eq. (9) $\rho_2(\mathbf{r}_1,\mathbf{r}_2)$ and $g(\mathbf{r}_1,\mathbf{r}_2)$ are the diagonal part of the second-order density matrix and the pair-correlation function with the electron interaction λ/r_{12} at full strength, $\lambda=1$. The second term of Eq. (6) is the kinetic contribution T_c to E_{xc} with the local potential $v_{kin}(\mathbf{r})$ being defined as follows:[16]

$$v_{kin}(\mathbf{r}_1)=\frac{1}{2}\int |\nabla_1\Phi(s_1,\mathbf{x}_2,\ldots,\mathbf{x}_N|\mathbf{r}_1)|^2 ds_1 d\mathbf{x}_2\cdots d\mathbf{x}_N = \frac{\nabla_1,\nabla_1\rho(\mathbf{r}_1',\mathbf{r}_1)|_{\mathbf{r}_1'=\mathbf{r}_1}}{2\rho(\mathbf{r}_1)}-\frac{[\nabla\rho(\mathbf{r}_1)]^2}{8\rho^2(\mathbf{r}_1)}. \tag{10}$$

In Eq. (10) $\Phi(s_1,\mathbf{x}_2,...,\mathbf{x}_N|\mathbf{r}_1)$ is the conditional probability amplitude[18] of the total wave function $\Psi(\mathbf{x}_1,\mathbf{x}_2,...,\mathbf{x}_N)(\{\mathbf{x}_i\}=\{\mathbf{r}_i,s_i\}$, $\{\mathbf{r}_i\}$ are the space and $\{s_i\}$ are the spin variables)

$$\Phi(s_1,\mathbf{x}_2,\ldots,\mathbf{x}_N|\mathbf{r}_1)=\frac{\Psi(\mathbf{x}_1,\ldots,\mathbf{x}_N)}{\sqrt{\rho(\mathbf{r}_1)/N}} \tag{11}$$

and $\rho(\mathbf{r}_1',\mathbf{r}_1)$ is the first-order density matrix for $\lambda=1$. $\Phi(s_1,\mathbf{x}_2,...,\mathbf{x}_N|\mathbf{r}_1)$ embodies all effects of electron correlation (exchange as well as Coulomb) in that its square is the probability distribution of the remaining $N-1$ electrons associated with positions $\mathbf{x}_2,...,\mathbf{x}_N$ when one electron is known to be at $\mathbf{r}_1$. v_{kin} can be interpreted[16] as a measure of how strongly the motion of the reference electron at $\mathbf{r}_1$ is correlated with other electrons in the system, in the sense that it reflects the magnitude of change in Φ with changing $\mathbf{r}_1$ (so it is a measure of the *change* in correlation hole with reference position $\mathbf{r}_1$). $v_{s,kin}$ is defined analogously to v_{kin} in terms of the Kohn–Sham functions,[16,19]

$$v_{s,kin}(\mathbf{r}_1)=\frac{1}{2}\int |\nabla_1\Phi_s(s_1,\mathbf{x}_2,\ldots,\mathbf{x}_N|\mathbf{r}_1)|^2 ds_1 d\mathbf{x}_2\cdots d\mathbf{x}_N = \frac{1}{2}\sum_{i=1}^{N}\left|\nabla_1\frac{\phi_i(\mathbf{r}_1)}{\rho^{1/2}(\mathbf{r}_1)}\right|^2, \tag{12}$$

$$\Phi_s(s_1,\mathbf{x}_2,\ldots,\mathbf{x}_N|\mathbf{r}_1)=\frac{\Psi_s(\mathbf{x}_1,\ldots,\mathbf{x}_N)}{\sqrt{\rho(\mathbf{r}_1)/N}}. \tag{13}$$

From Eqs. (1),(6),(7),(8) one can define ϵ_{xc} as follows:

$$\epsilon_{xc}(\mathbf{r})=\tfrac{1}{2}\,v_{xc}^{hole}(\mathbf{r})+v_{c,kin}(\mathbf{r}), \tag{14}$$

where

$$v_{c,kin}(\mathbf{r})=v_{kin}(\mathbf{r})-v_{s,kin}(\mathbf{r}). \tag{15}$$

Note that this definition of ϵ_{xc} is in terms of unique potentials that enter the Kohn–Sham equations and the effective potential for the density amplitude $\sqrt{\rho}$, and that have a clear physical interpretation. In the DFT literature an alternative definition of ϵ_{xc} is often used, in which it is expressed via an integral over the coupling parameter λ,[20,21]

$$\epsilon_{xc}(\mathbf{r}_1)=\frac{1}{2}\int\int_0^1 \frac{\rho(\mathbf{r}_2)[g^{\lambda}(\mathbf{r}_1,\mathbf{r}_2)-1]}{|\mathbf{r}_1-\mathbf{r}_2|}\,d\lambda\, d\mathbf{r}_2. \tag{16}$$

In this paper, however, we choose definition (14) as more convenient for our purpose, since in this case one does not need to know the dependence of g^{λ} on λ.

Equation (14) provides also a partitioning of v_{xc}. Taking the functional derivative Eq. (2) of Eq. (6) leads to the following expression for v_{xc}:

$$v_{xc}([\rho];\mathbf{r})=v_{xc}^{hole}([\rho];\mathbf{r})+v_{c,kin}([\rho];\mathbf{r})+v_{resp}([\rho];\mathbf{r}), \tag{17}$$

where

$$v_{resp}([\rho];\mathbf{r})=v_{xc}^{hole,resp}([\rho];\mathbf{r})+v_{c,kin}^{resp}([\rho];\mathbf{r}). \tag{18}$$

Here the potential $v_{xc}^{hole,resp}$ is an integral of the linear ''response'' of $g([\rho];\mathbf{r}_1,\mathbf{r}_2),\delta g([\rho];\mathbf{r}_1,\mathbf{r}_2)/\delta\rho(\mathbf{r}_3)$

$$v_{xc}^{hole,resp}([\rho];\mathbf{r}_3)=\frac{1}{2}\int \frac{\rho(\mathbf{r}_1)\rho(\mathbf{r}_2)}{|\mathbf{r}_1-\mathbf{r}_2|}\frac{\delta g([\rho];\mathbf{r}_1,\mathbf{r}_2)}{\delta\rho(\mathbf{r}_3)}\,d\mathbf{r}_1 d\mathbf{r}_2. \tag{19}$$

It is a measure of the sensitivity of the pair-correlation function to density variations. These density variations may be understood in the following way. If the density changes to (v-representable) $\rho+\delta\rho$, then according to the Hohenberg–Kohn theorem this changed density corresponds uniquely to an external potential $v_{ext}+\delta v_{ext}$. For the system with external potential $v_{ext}+\delta v_{ext}$ we have the corresponding Kohn–Sham system and the pair-correlation function $g([\rho+\delta\rho];\mathbf{r}_1,\mathbf{r}_2)$. So the derivative occurring in the response

potential (19) may be regarded as the linear response of g to density change $\delta\rho$ caused by potential change $\delta v_{\rm ext}$.

$v_{c,\rm kin}^{\rm resp}$ is the response of the potential $v_{c,\rm kin}$ to density variation

$$v_{c,\rm kin}^{\rm resp}([\rho];\mathbf{r}_1)=\int \rho(\mathbf{r}_2)\,\frac{\delta v_{c,\rm kin}([\rho];\mathbf{r}_2)}{\delta\rho(\mathbf{r}_1)}\,d\mathbf{r}_2. \tag{20}$$

From Eqs. (14),(17) a relation follows between $v_{\rm xc}$, and $\epsilon_{\rm xc}$,

$$v_{\rm xc}(\mathbf{r})=2\epsilon_{\rm xc}(\mathbf{r})-v_{c,\rm kin}(\mathbf{r})+v_{\rm resp}(\mathbf{r}). \tag{21}$$

In the next section a procedure will be presented for the numerical construction of $v_{\rm xc}$ and $\epsilon_{\rm xc}$ as well as their components from the correlated *ab initio* first- and second-order density matrices.

III. CONSTRUCTION OF $v_{\rm xc}$ AND $\epsilon_{\rm xc}$

To construct $v_{\rm xc}$, $\epsilon_{\rm xc}$ and their components, the first-order density matrix $\rho(\mathbf{r}',\mathbf{r})$, its diagonal part $\rho(\mathbf{r})$ and the diagonal part $\rho_2(\mathbf{r}_1,\mathbf{r}_2)$ of the second-order density matrix from *ab initio* calculations are used as the input functions. In our actual implementation[16] these functions are represented as matrices in the basis of the Hartree–Fock MO's. A scheme for the numerical construction consists of the following steps.[11]

(1) For a given grid $\{\mathbf{r}_i\}$ the Hartree potential $v_H(\mathbf{r}_i)$ is calculated from the correlated density $\rho(\mathbf{r})$, $v_{\rm kin}(\mathbf{r}_i)$ is calculated from $\rho(\mathbf{r}',\mathbf{r})$ via Eq. (10) and $v_{\rm xc}^{\rm hole}(\mathbf{r}_i)$ is calculated from $\rho(\mathbf{r})$ and $\rho_2(\mathbf{r}_1,\mathbf{r}_2)$ via Eq. (9). $v_{\rm kin}$ and $v_{\rm xc}^{\rm hole}$ are used for the analysis of $v_{\rm xc}$ and for the construction of $\epsilon_{\rm xc}$, while v_H and $v_{\rm xc}^{\rm hole}$ are used in the procedure of $v_{\rm xc}$ construction as components of the starting potential of electron interaction $v_{\rm el}^0$.

(2) $v_{\rm xc}(\mathbf{r}_i)$ and a set of KS orbitals $\{\phi_i(\mathbf{r})\}$ are obtained from the correlated $\rho(\mathbf{r})$ with an iterative procedure,[9] starting from some initial guess $v_{\rm el}^0$ for $v_{\rm el}$,

$$v_{\rm el}(\mathbf{r}_i)=v_H(\mathbf{r}_i)+v_{\rm xc}(\mathbf{r}_i). \tag{22}$$

At the mth iteration the KS equations (3) are solved with the potential $v_{\rm el}^m$,

$$v_{\rm el}^m(\mathbf{r}_i)=f_m(\mathbf{r}_i)v_{\rm el}^{m-1}(\mathbf{r}_i) \tag{23}$$

calculated from $v_{\rm el}^{m-1}$ of the previous iteration with the correction factor f_m, the latter being the ratio of the density ρ^{m-1} from the $(m-1)$th iteration and the given ρ,

$$f_m(\mathbf{r}_i)=\frac{\rho^{m-1}(\mathbf{r}_i)}{\rho(\mathbf{r}_i)}. \tag{24}$$

Then, ρ^{m-1} in Eq. (24) is replaced with ρ^m obtained at the mth iteration and this procedure continues until further iterations cease lowering the difference $|\rho^m(\mathbf{r}_i)-\rho(\mathbf{r}_i)|$ in the region of nonvanishing densities. Finally, $v_{\rm xc}(\mathbf{r}_i)$ is obtained by subtracting $v_H(\mathbf{r}_i)$ from the resulting potential (22). As was pointed out in Ref. 9, this iterative procedure is not guaranteed to converge. However, if it converges then its limit is unique as guaranteed by the Hohenberg–Kohn theorem applied to a noninteracting electron system.[22] In the calculations we have used a slightly modified form Eq. of (24),

$$f_m(\mathbf{r}_i)=\frac{\rho^{m-1}(\mathbf{r}_i)+a}{\rho(\mathbf{r}_i)+a}, \tag{25}$$

with $a=0.5$, which smooths out the effect of the remote exponential density tails on the procedure.

(3) $v_{c,\rm kin}(\mathbf{r}_i)$ is calculated from $v_{\rm kin}(\mathbf{r}_i)$, $\rho(\mathbf{r})$ and $\{\phi_i(\mathbf{r})\}$ via Eqs. (12)–(15) and $v_{\rm resp}(\mathbf{r}_i)$ is calculated by subtracting $v_{c,\rm kin}(\mathbf{r}_i)$ and $v_{\rm xc}^{\rm hole}(\mathbf{r}_i)$ from the constructed $v_{\rm xc}(\mathbf{r}_i)$.

(4) $\epsilon_{\rm xc}(\mathbf{r}_i)$ is obtained according to Eq. (14). Implementation of this scheme for the monohydrides LiH, BH, HF will be discussed in the next sections.

IV. DETAILS OF CALCULATIONS FOR LH, BH, HF

The monohydrides XH (X=Li, B, F) have been chosen because they form the simplest series of closed-shell molecules. For those molecules accurate empirical estimates of the Coulomb correlation energies E_c^e are available.[23] The correlated wave functions for XH have been obtained with singly and doubly excited configuration interaction (SDCI) calculations of the ground states at equilibrium distances R(Li–H)=3.015 a.u., R(B–H)=2.330 a.u., R(H–F)=1.733 a.u.. Calculations have been performed within the direct CI approach by means of the ATMOL package.[24]

A basis of contracted Gaussian functions[25] has been used with five s- and two p-type functions for H, seven s- and four p-type functions for Li, and seven s-, four p- and two d-type functions for B and F. For H an extra valence polarization d-function with the exponent $\alpha=1.0$ and for Li two such functions with the exponents $\alpha=0.36$ and $\alpha=0.15$ have been used. In order to better take into account the correlation effects for core electrons, this basis has been augmented for X with two localized polarization p- and two d-functions of the core size, whose exponents were set equal to those of the second most localized contracted s-function of the basis.[25] The increase in the absolute value of the correlation energy due to inclusion of core polarization functions amounts to 6% of E_c^e for LiH, 14% for BH, and 8% for HF, so that the SDCI calculations recover 93% of E_c^e for LiH, 90% for BH, and 78% for HF.

Calculation of $\rho(\mathbf{r}',\mathbf{r})$ and $\rho_2(\mathbf{r}_1,\mathbf{r}_2)$ from the SDCI wave functions with the subsequent construction of $v_{\rm xc}$, $\epsilon_{\rm xc}$ and their components has been performed in the same basis of MO's as the SDCI calculations by means of a special density functional extension[16,26] of the *ab initio* ATMOL package. Matrix elements of $v_{\rm el}^m$ in this basis have been calculated using a numerical integration with grids according to Ref. 27.

To obtain $v_{\rm xc}$ and $\{\phi_i\}$ via the procedure (22)–(25), two alternative initial potentials $v_{\rm el}^0$,

$$v_{\rm el}^0([\rho];\mathbf{r})=v_{\rm H}([\rho];\mathbf{r})+v_{\rm xc}^0([\rho];\mathbf{r}), \tag{26}$$

$$v_{\rm el}^0([\rho];\mathbf{r})=v_H([\rho];\mathbf{r})+v_{\rm xc}^{\rm hole}([\rho];\mathbf{r})+v_{\rm resp}^0([\rho];\mathbf{r}), \tag{27}$$

have been employed. In Eqs. (26), (27) v_H and $v_{\rm xc}^{\rm hole}$ are the rigorous Hartree potential and exchange-correlation hole potential calculated from the correlated $\rho(\mathbf{r})$ and $\rho_2(\mathbf{r}_1,\mathbf{r}_2)$, while $v_{\rm xc}^0$ and $v_{\rm resp}^0$ are the following approximations:[28]

$$v_{\rm xc}^0([\rho];\mathbf{r}) = v_{X\alpha}(\rho;\mathbf{r}) + 2\epsilon_x^B(\rho,|\nabla\rho|;\mathbf{r}) + 2\epsilon_c^{\rm VWN}(\rho;\mathbf{r}), \tag{28}$$

$$v_{\rm resp}^0([\rho];\mathbf{r}) = 0.382\sum_{i=1}^{N}\sqrt{\mu-\epsilon_i}\,\frac{|\phi_i(\mathbf{r})|^2}{\rho(\mathbf{r})}. \tag{29}$$

In Eq. (28) $v_{X\alpha}$ is the exchange-correlation $X\alpha$ potential,[29] ϵ_x^B is the exchange energy density gradient correction of Becke,[30] and $\epsilon_c^{\rm VWN}$ is the local density approximation (LDA) of Vosko, Wilk, and Nusair[31] for the correlation energy density. The parameter α of $v_{X\alpha}$ is chosen from the following fitting condition:

$$[-\tfrac{1}{2}\nabla^2 + v_{\rm ext}(\mathbf{r}) + v_{\rm el}^0(\mathbf{r})]\phi_N(\mathbf{r}) = -I_p\phi_N(\mathbf{r}), \tag{30}$$

where ϕ_N is the highest occupied Kohn–Sham molecular orbital (HOMO) and I_p is the experimental ionization energy of the molecule. The Kohn–Sham calculation with this optimized potential may also be used to construct $v_{\rm resp}^0$ of Eq. (29), which is the KS orbital dependent approximation[28] for $v_{\rm resp}$ with ϵ_i being the energy of the KS orbital ϕ_i and μ being the Fermi level of a given system, which is equal to the energy of the HOMO $\mu=\epsilon_N$. Both potentials (26) and (27) have a proper long-range Coulombic asymptotics $v_{\rm el}^0 \to -(Z-1)/|\mathbf{r}|$.

For the lighter monohydrides LiH and BH the results obtained depend only slightly on the type of the initial guess used, with Eq. (26) providing a somewhat better final HOMO energy. This is probably due to the for this property ''perfect'' starting potential [cf. Eq. (30)]. After 45–50 iterations the procedure (22)–(25) has reached its saturation state, with no further discernible change of results. The densities obtained agree with the correlated ρ within 0.1% in the region of nonvanishing densities. Similar accuracy for e_N (and ρ) may probably be obtained with the starting potential of Eq. (27) by varying the constant in $v_{\rm resp}^0$ [Eq. (29)] so as to start with the accurate $e_N=-I_p$, but we are satisfied with the solution obtained with the initial guess (26). The results obtained with this starting potential will be presented in the next section.

For the heavier HF system the initial potential (26) appears to overestimate substantially the attractive character of $v_{\rm xc}$ near the F nucleus. The subsequent iterative procedure has not been able to remove this defect and it has not reached its saturation state even after 100 iterations. The resulting $v_{\rm xc}$ appears to be very close to $v_{\rm xc}^{\rm hole}$ near the F nucleus. Since it is known[12,28] that the response potential $v_{\rm resp} = v_{\rm xc} - v_{\rm xc}^{\rm hole} - v_{c,\rm kin}$ is fairly large and positive in the $1s$ region (see Fig. 8 below), and $v_{c,\rm kin}$ is much smaller (cf. Fig. 7), $v_{\rm xc}$ is obviously somewhat deficient. On the other hand, with the initial guess (27) for HF, which does build in correctly this repulsive term in the $1s$ region [cf. Eq. (29)] from the start, the procedure did approach its saturation state with the resulting $v_{\rm xc}$ being appreciably less attractive than $v_{\rm xc}^{\rm hole}$ near the F nucleus. The results for HF obtained with the initial guess (27) will be presented in the next sections.

TABLE I. Kohn–Sham energy characteristics (a.u.).

	LiH	BH	HF
$\epsilon_{\rm HOMO}$	−0.284	−0.359	−0.585
$-I_p$	−0.283	−0.359	−0.589
T_s	8.001	25.153	100.072
$T_{\rm HF}$	7.993	25.119	100.027
$T^{\rm CI}$	8.058	25.252	100.309
$T_c^{\rm CI}$	0.057	0.099	0.237
T_c^e	0.061	0.110	0.304
$T_c^{\rm CI}/T_{c,\rm HF}^{\rm CI}$	0.88	0.75	0.84
ΔT_s	0.061	0.093	0.102
ΔT_c	0.023	0.012	0.050

V. KOHN–SHAM ENERGY CHARACTERISTICS

Table I presents various energy characteristics for the KS orbitals $\{\phi_i(\mathbf{r})\}$, which have been obtained with the procedure (22)–(25). The first is the HOMO energy ϵ_N. According to Refs. 33–36, an accurate HOMO energy ϵ_N is equal to minus the ionization potential of the system I_p and ϵ_N values obtained for XH are indeed close to the experimental $-I_p$ values (see Table I). In this respect it is informative to consider the evolution we observed of ϵ_N calculated for LiH and BH during the cycles of the iteration procedure. Starting from the value $\epsilon_N^0=-I_p$ [because of the fitting condition (30)], ϵ_N departs from $-I_p$ at the first few iterations with simultaneous lowering of the calculated KS kinetic energy T_s and then goes back to the value $-I_p$ at the subsequent iterations.

Table I also presents the kinetic energy of the KS system T_s,

$$T_s = -\frac{1}{2}\sum_{i=1}^{N}\int \phi_i^*(\mathbf{r})\nabla^2\phi_i(\mathbf{r})d\mathbf{r} \tag{31}$$

and the kinetic part of the exchange-correlation energy T_c, where we indicate the fact that we are dealing with an approximation to this quantity by a CI calculation by way of the superscript CI,

$$T_c^{\rm CI} = T^{\rm CI} - T_s = \int \rho(\mathbf{r})v_{c,\rm kin}(\mathbf{r})d\mathbf{r}. \tag{32}$$

Since the DFT definition of correlation energy deviates from the conventional one, which is always with respect to the Hartree–Fock energy as the reference, we will denote the conventional quantities with the subscript HF,

$$E_{c,\rm HF} = E - E^{\rm HF},$$
$$T_{c,\rm HF} = T - T^{\rm HF}. \tag{33}$$

Due to the virial theorem these exact quantities are equal

$$\frac{T_{c,\rm HF}}{E_{c,\rm HF}} = -1. \tag{34}$$

The approximation to the exact conventional correlation energy that we obtain from our SDCI calculation, $E_{c,\rm HF}^{\rm CI}$, may

be compared to the known exact values,[23,32] to obtain improved estimates from the CI approximations to $T_{c\mathrm{HF}}$ and to T_c,

$$T^e_{c,\mathrm{HF}} = T^{\mathrm{CI}}_{c,\mathrm{HF}} \frac{E_{c,\mathrm{HF}}}{E^{\mathrm{CI}}_{c,\mathrm{HF}}},$$

$$T^e_c = T^{\mathrm{CI}}_c \frac{E_{c,\mathrm{HF}}}{E^{\mathrm{CI}}_{c,\mathrm{HF}}}. \tag{35}$$

The correction factors are 1.075, 1.11, and 1.28 for LiH, BH, and FH, respectively. The extrapolated values for T_c, denoted with a superscript e (cf. Table I), are still approximations for two reasons. In the first place, applying the correction factor deduced from the correlation energies (exact and CI) to just the kinetic part of the correlation energy is only allowed if the virial theorem would also hold for the approximate CI, whereas it will only hold exactly for a full CI. In the second place, the correction factor is not necessarily equal for $T^{\mathrm{CI}}_{c,\mathrm{HF}}$ and T^{CI}_c. In particular, the extrapolation of T_c will be dubious in systems that are not good Hartree–Fock cases, i.e., where a single determinant is not a good first order approximation to the wave function, such as a dissociating molecule. In such a case T_s may differ strongly from T^{HF}, cf. Table II in Ref. 16.

It is interesting to consider in the present series of molecules, where Hartree–Fock *is* a reasonable first approximation, what actually the difference is between T_s and T_{HF}. The KS kinetic functional $T_s[\rho]$ minimizes the kinetic energy for a Kohn–Sham determinant with the density constrained to the correlated density ρ. It is well known that the correlated density is more contracted around the nuclei than the Hartree–Fock density, which is extremely so in poor Hartree–Fock cases like dissociating H_2.[16,46] Due to this contraction effect of correlation, the minimal energy T_s is still higher than T^{HF}. Although the difference is not large percentage wise (see Table I), it is not negligible on the scale of the difference between T^{CI} and T_s, i.e., T_c. As a result, the ratio $T^{\mathrm{CI}}_c/T^{\mathrm{CI}}_{c,\mathrm{HF}}$ is consistently lower than 1 for XH ranging from 0.75 for BH to 0.88 for LiH. We may expect this ratio to be closer to 1 in the corresponding atoms, since the atoms X are closer to the limiting case of tightly bound, good Hartree–Fock systems.

One can study the effect of bond formation on the kinetic functionals by comparison of T_s and T^e_c values obtained at the equilibrium X–H distance with the sum of atomic values for X and H. For the one-electron H atom $T^e_c(\mathrm{H})=0$ and the KS system coincides with the exact one, so that, according to the virial theorem, $T_s(\mathrm{H})$ is equal to minus the total energy of the H atom $T_s(\mathrm{H})=0.5$ a.u. Taking $T_s(\mathrm{X})$ values from Ref. 37 and extracting $T^e_c(\mathrm{X})$ values from the data reported in this reference, we obtain the differences

$$\Delta T_s = T_s(\mathrm{XH}) - T_s(\mathrm{X}) - 0.5, \tag{36}$$

$$\Delta T_c = T^e_c(\mathrm{XH}) - T^e_c(\mathrm{X}), \tag{37}$$

which are presented in Table I. We note that the atomic data in Ref. 37 are approximate since the atoms are open shell systems that have been treated using sherical averaging.

For the series XH (X=Li, B, F) the difference ΔT_s is a positive quantity, which increases monotonically from 0.061 a.u. for LiH to 0.093 a.u. for BH and to 0.102 a.u. for HF. The positive sign of ΔT_s is in line with the positive sign of the exact as well as Hartree–Fock values for the kinetic energy change upon bond formation. It reflects contraction of the KS orbitals occurring at bond distances close to R_e. This can be understood, if we rewrite the expression (31) for T_s in the gradient form,[1]

$$T_s = \frac{1}{2}\sum_{i=1}^{N} \int |\nabla \phi_i(\mathbf{r})|^2 d\mathbf{r}. \tag{38}$$

The more localized the KS orbitals are, the higher are their gradients, which leads, according to Eq. (38) to increase of T_s. The energetical effect of the orbital contraction increases with increasing nuclear charge of the X atom. The kinetic energy effects due to bond formation, in particular the lowering of the kinetic energy at long distances and the orbital contraction and concomitant kinetic energy rise at $R \approx R_e$ have been studied in the classical papers by Ruedenberg *et al.* on H_2^+ and H_2.[38,39] An analysis of kinetic energy effects for individual Kohn–Sham orbitals describing various bond types (σ and π) at long and short distances has been given in Ref. 40.

The difference ΔT_c reflects the effect of bond formation on the kinetic part of the correlation functional. Unlike ΔT_s, it changes nonmonotonically in the series XH; ΔT_c is minimal for BH (0.012 a.u.), it is larger for LiH (0.023 a.u.), and it has the largest value 0.050 a.u. for HF. Note the same trend for the difference $\Delta E_{c\mathrm{HF}} = E_{c,\mathrm{HF}}(\mathrm{XH}) - E_{c,\mathrm{HF(X)}}$ of the conventional total correlation energies,[23] which have the values 0.038, 0.028, and 0.064 a.u. for LiH, BH, and HF, respectively. This is not surprising, because the conventional exact quantities $T_{c,\mathrm{HF}}$ and $E_{c,\mathrm{HF}}$ are equal on account of the virial theorem, and T_c is roughly proportional to $T_{c,\mathrm{HF}}$ for both atomic and molecular systems considered.

VI. POTENTIALS AND ENERGY DENSITIES

In Figs. 1–3 the molecular Kohn–Sham exchange-correlation potentials v_{xc} constructed for the series XH (X =Li, B, F) are compared with the potentials of the exchange-correlation hole $v^{\mathrm{hole}}_{\mathrm{xc}}$. The potentials are plotted along the bond axis, as functions of the distance z from the bond midpoint. In all cases v_{xc} is everywhere less attractive than the corresponding $v^{\mathrm{hole}}_{\mathrm{xc}}$. This is an anticipated trend since, according to Eq. (17), v_{xc} can be obtained by addition of v_{resp} and $v_{c,\mathrm{kin}}$ to $v^{\mathrm{hole}}_{\mathrm{xc}}$, and the former potentials are expected[12,16,42] to be mainly repulsive.

The form of v_{xc} resembles that of $v^{\mathrm{hole}}_{\mathrm{xc}}$, for instance, both potentials have a deep well around the nucleus X. This is simply due to the fact that at positions $\mathbf{r}$ within the $1s$ shell the exchange hole surrounding $\mathbf{r}$ is very close to minus the $1s$ density, leading to a strongly attractive potential. Still, there exists a significant difference between v_{xc} and $v^{\mathrm{hole}}_{\mathrm{xc}}$; while $v^{\mathrm{hole}}_{\mathrm{xc}}$ is a rather smooth potential, v_{xc} displays a characteristic structure. The most visible features of v_{xc} are the local maxima (intershell peaks) between the core and valence

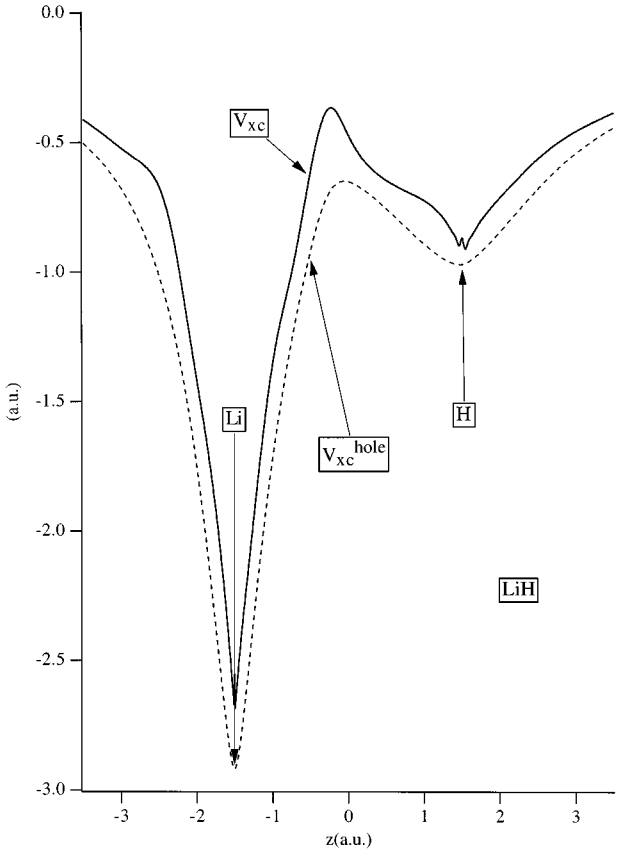

FIG. 1. Kohn–Sham exchange-correlation potential and the potential of the exchange-correlation hole for LiH.

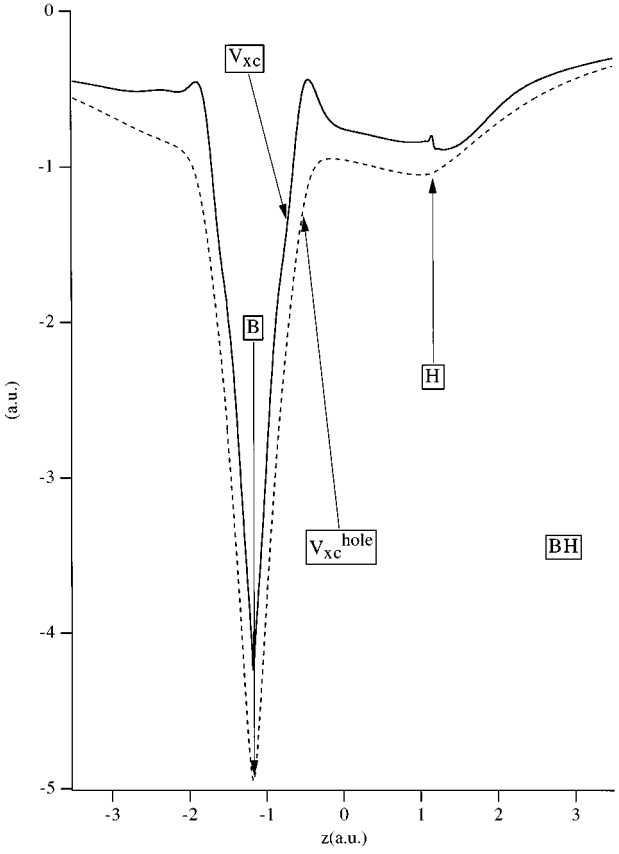

FIG. 2. Kohn–Sham exchange-correlation potential and the potential of the exchange-correlation hole for BH.

regions. One can see them most clearly on the outer sides of the B and F atoms with the maxima of the peaks being placed at $z=-1.90$ a.u. and $z=-1.22$ a.u., respectively. The outer-side intershell peak is more pronounced in the case of the F atom in the HF molecule, while it is less pronounced for B and it completely disappears for Li in the LiH molecule. The same trend is observed for the intershell peaks of individual atoms X (see Figs. 2 and 3 of Ref. 37). Analogous peaks are displayed on the inner, bonding sides of X in BH and HF with the maxima at $z=-0.45$ a.u. and $z=-0.50$ a.u., respectively. v_{xc} for LiH also exhibits a peak in the bonding region, but its maximum $z=-0.22$ is closer to the bond midpoint and this peak seems to be caused by a combination of various correlation effects (see the discussion below).

v_{xc} displays also features in the valence region, which can be related to the heteropolar nature of the diatomic bonds, leading to anionic atoms $F^{\delta-}$ in HF and $H^{\delta-}$ in LiH. Local wells in v_{xc} are discernable that ''attract'' electrons to the electronegative atom. For HF this well surrounds the F core just beyond the intershell peak and where the bond axis intersects with the well local minima in v_{xc} are visible in Fig. 3 at $z=-1.39$ a.u. and $z=-0.31$ a.u. For LiH, this well spans the region of the H atom (see Fig. 1) with the minimum placed at the H nucleus (we neglect the small wiggle at the H nucleus, which probably is an artefact of the iterative procedure of v_{xc} construction). These wells favor accumulation of the electron density on the more electronegative atoms F (in HF) and H (in LiH), thus providing the ionic patterns of the electron distribution $H^{\delta+}$–$F^{\delta-}$ and $Li^{\delta+}$–$H^{\delta-}$. For BH, a molecule with a more covalent type of bonging, v_{xc} exhibits a more ''covalent'' pattern, having a flat shape in the bonding region (see Fig. 2).

In Figs. 4–6 the exchange-correlation energy density ϵ_{xc} [as defined in Eq. (14)] is plotted for the series XH together with its potential $\frac{1}{2}v_{\mathrm{xc}}^{\mathrm{hole}}$ and kinetic $v_{c,\mathrm{kin}}$ components. It is not surprising, that the form of ϵ_{xc} is determined primarily by that of its potential component. While $v_{c,\mathrm{kin}}$ represents a Coulomb correlation effect, $v_{\mathrm{xc}}^{\mathrm{hole}}$ represents also the exchange, a dominating part of the total electronic exchange-correlation. Still, a proper account of the pure Coulomb correlation effect on both potential and kinetic functionals, embodied in the Coulomb hole potential v_c^{hole} and in $v_{c,\mathrm{kin}}$, is important for an adequate description of molecular systems, especially for one-electron properties of valence electrons and for bonding properties.

In all cases ϵ_{xc} has a deep and rather sharp well around the X nucleus, caused by $\frac{1}{2}v_{\mathrm{xc}}^{\mathrm{hole}}$, i.e., by the exchange hole in the $1s$ shell, see above. However, the form of ϵ_{xc} in the region of the H atom changes substantially within the series XH. For LiH ϵ_{xc}, just as its dominating component $\frac{1}{2}v_{\mathrm{xc}}^{\mathrm{hole}}$, has a distinct well around the H nucleus, while for BH such a well becomes very shallow and for HF it completely dis-

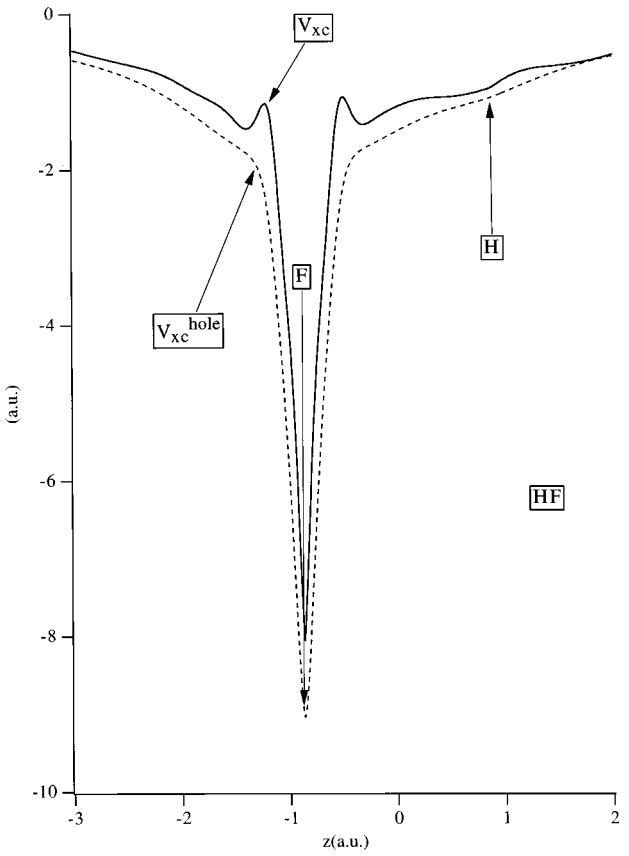

FIG. 3. Kohn–Sham exchange-correlation potential and the potential of the exchange-correlation hole for HF.

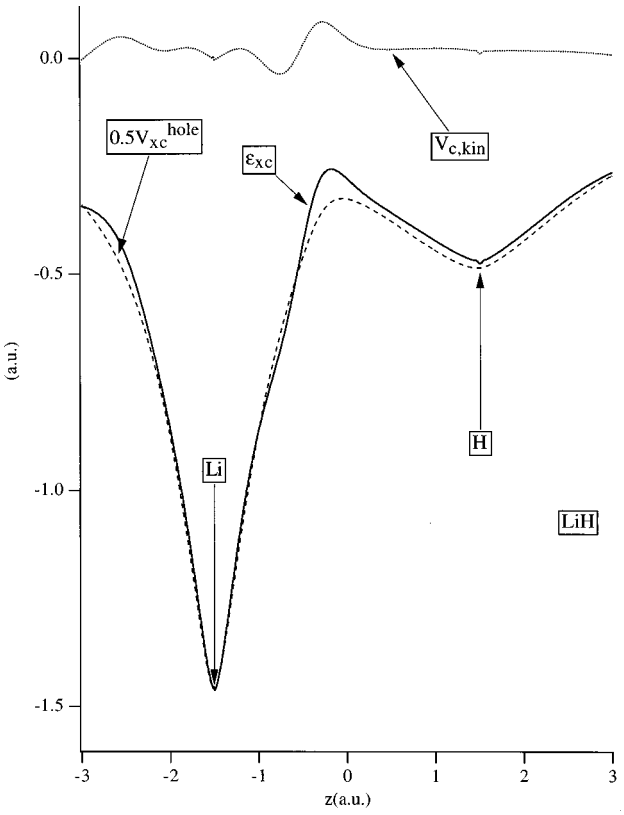

FIG. 4. Exchange-correlation energy density and its kinetic and potential components for LiH.

appears. This trend reflects the above-mentioned effect of a different ionicity of the H atom on $v_{\rm xc}^{\rm hole}$, which is also the dominating component of $v_{\rm xc}$.

The kinetic part $v_{c,\rm kin}$ of the exchange-correlation energy density is small compared to $\epsilon_{\rm xc}$, due to the large exchange contribution to that quantity. Nevertheless, addition of $v_{c,\rm kin}$ to $\frac{1}{2}v_{\rm xc}^{\rm hole}$ produces some structure in $\epsilon_{\rm xc}$. One may mention the distinct peak of $\epsilon_{\rm xc}$ in the bond midpoint region of LiH (see Fig. 4) or its small intershell peak on the outer side of the B atom in BH (see Fig. 5). Still, because of the small amplitude of $v_{c,\rm kin}$, $\epsilon_{\rm xc}$ is everywhere rather close to $\frac{1}{2}v_{\rm xc}^{\rm hole}$, being less negative than $\frac{1}{2}v_{\rm xc}^{\rm hole}$ for the majority of z values. For larger $|z|$ values both $\epsilon_{\rm xc}$ and $\frac{1}{2}v_{\rm xc}^{\rm hole}$ approach the Coulombic asymptotics $-0.5/|z|$.

In Figs. 7(a) and 7(b) the potentials $v_{c,\rm kin}$ are presented. In order to make the comparison more clear, in Fig. 7(a) the plot of $v_{c,\rm kin}$ vs the scaled coordinate $z'=1.29z$ (1.29 is the bond length ratio for LiH and BH) for BH is compared with $v_{c,\rm kin}(z)$ for LiH, so that the nuclear positions in both plots coincide. Analogously, in Fig. 7(b) the plot $v_{c,\rm kin}(z')$, $z'=1.34z$ for HF is compared with $v_{c,\rm kin}(z)$ for BH.

Figures 7(a) and 7(b) show that $v_{c,\rm kin}$ is an oscillating function in the region of the atom X, the oscillations tend to become more contracted with increasing atomic number of X. Apart from this contraction, $v_{c,\rm kin}$ displays some characteristic patterns. Its most visible features are the positive peaks in the intershell regions. One can see them, for example, on the inner, bonding side of the X atom with the maxima of the peaks being placed at $z=-0.27$ for LiH and $z'=-0.65$ for BH in Fig. 7(a), and at $z=-0.50$ for BH and $z'=-0.74$ for HF in Fig. 7(b). The peaks are higher and closer to the nucleus for the heavier X, the latter feature illustrates the abovementioned contraction of the $v_{c,\rm kin}$ oscillations. Note, that scaling of the z coordinate reduces the visual effect of contraction, so that for the real, unscaled coordinate z the contraction of oscillations is stronger.

Closer to the X nucleus, the peaks of $v_{c,\rm kin}$ are replaced with negative wells of a lower amplitude (except for the sharp peak at the nucleus mentioned before). In the bonding region $v_{c,\rm kin}$ has a smoother behavior. It decreases in the direction of the H atom, passing through a small local maximum in the bonding region. In this region $v_{c,\rm kin}$ is somewhat reminiscent (especially for HF) of the corresponding potential for the H_2 molecule at the equilibrium distance, which has been constructed in Ref. 16.

This complicated behavior of $v_{c,\rm kin}$ reflects the fact that, according to its definition (15), the relatively small $v_{c,\rm kin}(\mathbf{r}_1)$ is a difference of two larger potentials, $v_{\rm kin}(\mathbf{r}_1)$ and $v_{s,\rm kin}(\mathbf{r}_1)$. In its turn, the latter difference is determined according to Eqs. (10), (12) by the integrated difference of the conditional amplitude gradients $|\nabla_1\Phi(s_1,\mathbf{x}_2,...,\mathbf{x}_N|\mathbf{r}_1)|^2$ and $|\nabla_1\Phi_s(s_1,\mathbf{x}_2,...,\mathbf{x}_N|\mathbf{r}_1)|^2$ or, in other words, by the relative sensitivity of the total exchange-correlation hole and the pure exchange (Fermi) hole in the distribution of other electrons

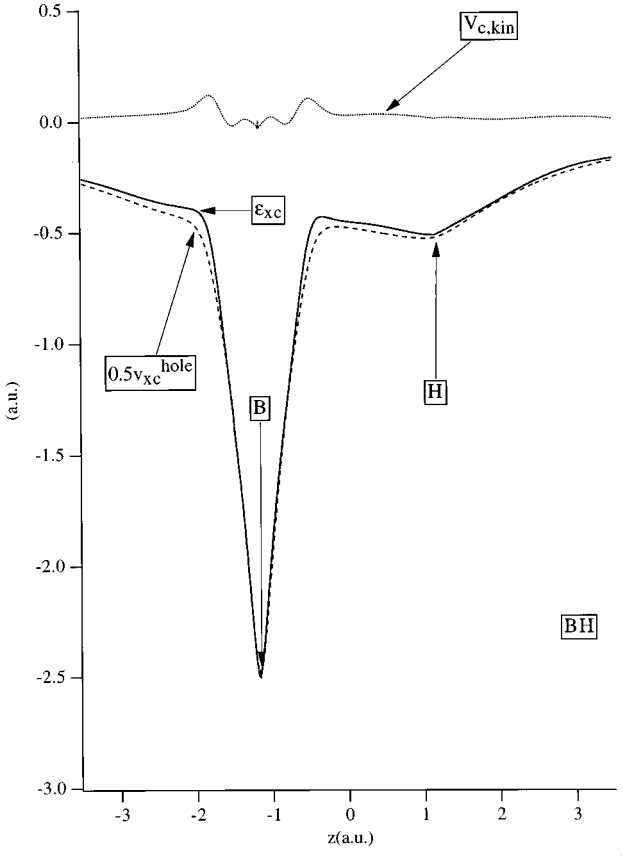

FIG. 5. Exchange-correlation energy density and its kinetic and potential components for BH.

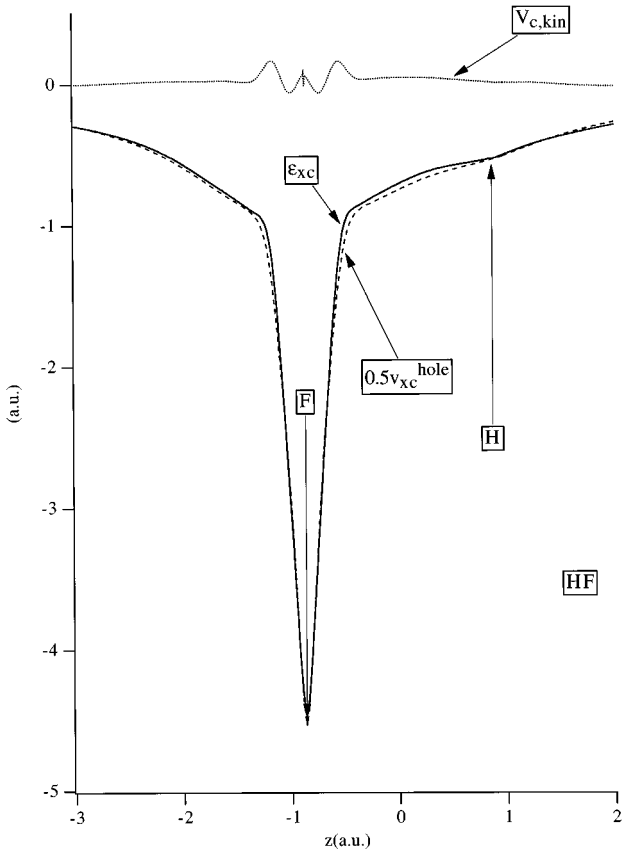

FIG. 6. Exchange-correlation energy density and its kinetic and potential components for HF.

to the displacement of the reference electron from $\mathbf{r}_1$. If the exchange-correlation hole associated with $\Phi(s_1,\mathbf{x}_2,...,\mathbf{x}_N|\mathbf{r}_1)$ has a more substantial change of its form than the Fermi hole associated with $\Phi_s(s_1,\mathbf{x}_2,...,\mathbf{x}_N|\mathbf{r}_1)$, $v_{c,\mathrm{kin}}(\mathbf{r}_1)$ will be positive and it will be close to zero if there is no or little Coulomb correlation or even negative if the Coulomb hole variation counteracts the Fermi hole variation so as to produce a smaller sensitivity to the reference position of the total hole than just the Fermi hole. Note, that in the exchange-only case only electrons with the same spin as that of the reference electron respond to its displacement. On the other hand, in the exchange-correlation case electrons with both the same and opposite spins change their distribution with the changing $\mathbf{r}_1$. Because of this, $v_{c,\mathrm{kin}}(\mathbf{r}_1)$ is positive in the main regions.

The maximum of $v_{c,\mathrm{kin}}$ in the $1s-2s$ intershell region can be interpreted in the following way. It is well known that the intershell peak in v_{kin} reflects the fact that the Fermi hole ''jumps'' from one shell to another accompanying the reference electron when it crosses the intershell border.[43–45,16,46] Less is known about the Coulomb hole. From the results of Ref. 46 it is clear that when the reference position is within a shell (like the $1s$ in He) the hole will have a contractive shape when the $\mathbf{r}_{\mathrm{ref}}$ is in the outer part; spherical, negative around $r=|\mathbf{r}_{\mathrm{ref}}|$, positive closer to the nucleus. When the reference position is at intermediate positions in the shell, the hole has a polarization shape; negative around $\mathbf{r}_{\mathrm{ref}}$, positive at the other side of the nucleus. When $\mathbf{r}_{\mathrm{ref}}$ is close to the nucleus, the hole acquires an expansive shape; spherical, negative around the nucleus and $\mathbf{r}_{\mathrm{ref}}$, positive in the outer region. When the reference position moves (e.g., in Ne) out of the $2s$ region into the $1s$ shell, the Coulomb hole almost disappears from the $2s$ region and becomes purely polarizationlike within the $1s$ shell (Fig. 3.3 of Ref. 46). This Coulomb hole behavior enhances the ''jump'' of the exchange hole from $2s,2p$ character to $1s$ character, which explains the positive peak in $v_{c,\mathrm{kin}}$ in the $2s-1s$ border region. When moving closer to the nucleus the hole stabilizes to a Fermi part that is just minus the $1s$ density, and a Coulomb part that is polarization like, and $v_{c,\mathrm{kin}}$ becomes small (actually somewhat negative). Moving still closer to the nucleus we observe again (smaller) peaks at both sides of the nucleus, which become larger and considerably closer to the nucleus in the series Li, B, F (in F they nearly coalesce). While the Fermi hole is stable at these reference positions, we conjecture that these peaks are related to the change in Coulomb hole from polarization to expansion shape. We have no explanation for the sharp dip at the nucleus, which may be an artefact of our procedure for constructing v_{xc}, or may be caused by the unphysical Gaussian shape of our CI density at the nucleus.

The behavior of $v_{c,\mathrm{kin}}$ in the bonding region reflects the

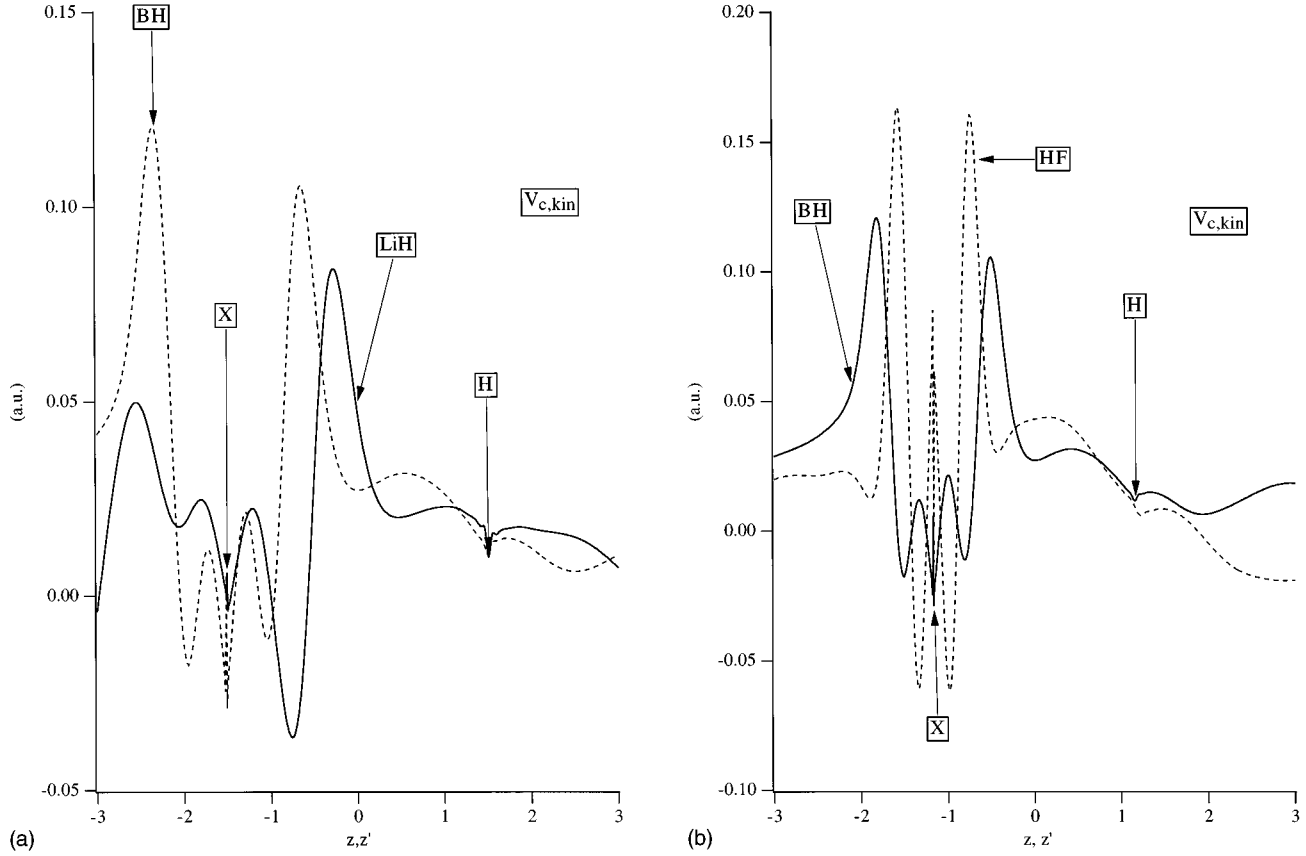

FIG. 7. Comparison of the potentials $v_{c,\mathrm{kin}}$ for (a) LiH and BH; (b) BH and HF.

effect of the left–right correlation of electrons of a single bond X–H. When the reference electron crosses the bond midpoint, another electron has to switch from one atom to the other due to the left–right correlation of electrons of a single bond X–H. As a consequence, a bond midpoint peak is expected to appear[16] in $v_{c,\mathrm{kin}}$. Since there is no analogous exchange effect, $v_{c,\mathrm{kin}}$ is definitely positive in this region with a small local maximum near the bond midpoint. However, as was shown in Ref. 16 for the case of the H_2 molecule, the effect is small at the equilibrium geometry and only for the dissociating molecule, where the left–right correlation is strengthened by the strong near-degeneracy effect, $v_{c,\mathrm{kin}}$ developes a relatively high bond midpoint peak.

In Fig. 8 the response potentials v_{resp} are plotted, which have been obtained by subtraction of $v_{c,\mathrm{kin}}$ and $v_{\mathrm{xc}}^{\mathrm{hole}}$ from v_{xc}. Just as in the case of $v_{c,\mathrm{kin}}$, $v_{\mathrm{resp}}(z')$, $z'=1.29z$ and $v_{\mathrm{resp}}(z'')$, $z''=1.74z$ are plotted for BH and HF respectively. As was established in Ref. 12 within the exchange-only OPM model,[13,14,15] the atomic $v_x^{\mathrm{hole,resp}}$ is a repulsive potential, which has the characteristic form of a step function with the steps representing individual electronic shells. For example, for atoms of the second period with a $1s$ core $v_x^{\mathrm{hole,resp}}$ has just one step with the higher plateau for the $1s$ electrons and with a rather steep descent to low values in the region of the $2s,2p$ electrons. In Ref. 42 it has been shown within the generalization of the exchange-only Krieger–Li–Iafrate approximation[47] that the steps of $v_x^{\mathrm{hole,resp}}$ originate from the corresponding stepped structure of the derivative $\delta g_x(\mathbf{r}_1,\mathbf{r}_2)/\delta\rho(\mathbf{r}_3)$ [see Eq. (19)] as a function of $\mathbf{r}_3$ and an expression has been obtained for individual step heights in terms of the energetical characteristics of the corresponding shell.

By construction, v_{resp} presented in this paper contains not only the exchange component $v_x^{\mathrm{hole,resp}}$, but also the correlation components $v_c^{\mathrm{hole,resp}}$ and $v_{c,\mathrm{kin}}^{\mathrm{resp}}$ [see Eq. (20)]. One can see from Fig. 8 that for all systems the v_{resp} obtained are everywhere positive, repulsive potentials. Though far from perfect, the one-step structure can be recognized for v_{resp} of BH with higher values for the core electrons and lower values for other electrons. The step pattern is disturbed, mainly, by the cusps and wiggles of v_{resp} near the nuclei. In particular, v_{resp} for HF has an especially deep cusp near the F nucleus. One of the possible reasons for these features can be the inclusion of the correlation effects. Another reason can be the performance of the numerical procedure of v_{xc} construction. Because of the singularity of the derivative of ρ at nuclei, it appears to be somewhat difficult, in general, to achieve high numerical accuracy of the KS solution in the core regions.[4,9,10,11]

Nevertheless, Fig. 8 represents a reasonable trend for v_{resp} in the series XH. For the heavier X atoms the step exhibits a definite contraction (which should be more pronounced for the real, unscaled coordinate z) and the height of the step $\delta\epsilon$ increases in accordance with its rough estimate[28]

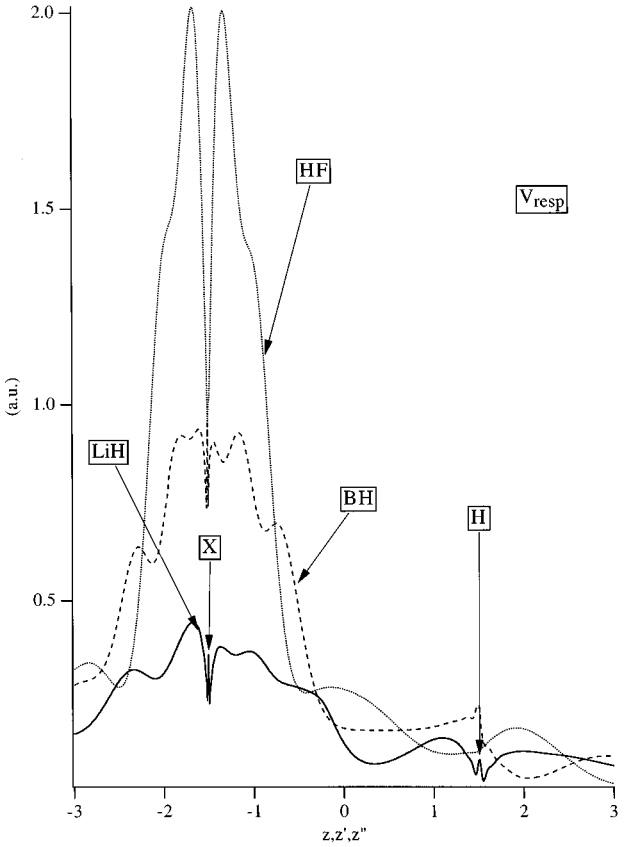

FIG. 8. Comparison of the potentials v_{resp}.

$$\delta\epsilon = 0.38\sqrt{\epsilon_{\mathrm{HOMO}} - \epsilon_{1s}}, \tag{39}$$

where ϵ_{1s} is the energy of the core orbital.

To sum up, the analysis of v_{xc} performed in this section shows the role of its various components. While $v_{\mathrm{xc}}^{\mathrm{hole}}$ determines the general form of v_{xc}, v_{resp} and $v_{c,\mathrm{kin}}$ provide an additional structure on top of that of $v_{\mathrm{xc}}^{\mathrm{hole}}$. Each component of v_{xc} displays its own characteristic structure, $v_{\mathrm{xc}}^{\mathrm{hole}}$ has wells around the X nuclei and around the H nucleus of the $H^{\delta-}$ anionic atom of LiH $v_{c,\mathrm{kin}}$ has peaks in the intershell and bond midpoint regions, while v_{resp} displays steplike structure. The structure of v_{xc} and its components reflects effects of electronic structure and electron correlation, such as the ionicity of XH molecules and the variation of the form of the exchange-correlation hole in various molecular regions. $v_{\mathrm{xc}}^{\mathrm{hole}}$ and $v_{c,\mathrm{kin}}$, the ''energetical'' parts of v_{xc}, yield the exchange-correlation energy density, thus defining the local energetical effect of the electron correlation.

VII. CONCLUSIONS

In this paper the molecular Kohn–Sham exchange-correlation potentials v_{xc} and the energy densities ϵ_{xc} have been constructed from *ab initio* first- and second-order density matrices for the series XH (X=Li, B, F). Comparison of the molecular values of the KS kinetic functionals T_s and T_c obtained in this paper with the atomic ones obtained in Ref. 37 has revealed the effect of bond formation on these functionals. The energies of the highest occupied KS MO calculated with v_{xc} reproduce the experimental ionization energies of XH.

The structure of v_{xc} and ϵ_{xc} has been analyzed in terms of their components $v_{\mathrm{xc}}^{\mathrm{hole}}$, $v_{c,\mathrm{kin}}$ and v_{resp}. The form of v_{xc} and ϵ_{xc} is determined by a combination of the characteristic features of their components, namely, the wells of $v_{\mathrm{xc}}^{\mathrm{hole}}$, the peaks of $v_{c,\mathrm{kin}}$ and (in the case of v_{xc}) the stepped-like patterns of v_{resp}. The relation of these features with various effects of electronic structure and electron correlation has been discussed. Anionic nature of atomic fragments $H^{\delta-}$ in the LiH molecule and $F^{\delta-}$ in the HF molecule manifests itself through the formation of local wells of v_{xc} in the corresponding regions.

The present results have shown sensitivity of the molecular KS solution obtained via the iterative procedure (22)–(25) to the starting potential v_{el}^{0}. This is especially true for the regions near the nuclei. The stability of the procedure also appears to decrease when going from the lighter LiH and BH molecules to the heavier HF molecule. One of the possible reasons of this is the local nature of the simple updating formula (23), (24) for the potential of electron interaction v_{el}. According to this formula, the change of potential at the mth iteration $\Delta v_{\mathrm{el}}(\mathbf{r}) = v_{\mathrm{el}}^{m}(\mathbf{r}) - v_{\mathrm{el}}^{m-1}(\mathbf{r})$ depends explicitly only on the local density difference $\Delta\rho(\mathbf{r}) = \rho^{m-1}(\mathbf{r}) - \rho(\mathbf{r})$ and the local ratio $v_{m-1}(\mathbf{r})/\rho(\mathbf{r})$,

$$\Delta v_{\mathrm{el}}(\mathbf{r}) = \frac{v_{\mathrm{el}}^{m-1}(\mathbf{r})}{\rho(\mathbf{r})}\,\Delta\rho(\mathbf{r}). \tag{40}$$

In this sense one can expect a better performance of an integral formula

$$\Delta v_{\mathrm{el}}(\mathbf{r}) = \int \chi_s^{-1}(\mathbf{r},\mathbf{r}')\Delta\rho(\mathbf{r}')\,d\mathbf{r}', \tag{41}$$

according to which the local potential change $\Delta v_{\mathrm{el}}(\mathbf{r})$ has a proper nonlocal dependence on $\Delta\rho(\mathbf{r}')$ in all points $\mathbf{r}'$. In Eq. (41) χ_s^{-1} is the inverse static density response function. In Ref. 3 it was proposed to use Eq. (41) for the construction of v_{xc} and in Refs. 7, 48 the corresponding scheme of calculations has been developed. Unfortunately, calculation of $\chi_s^{-1}(\mathbf{r}, \mathbf{r}')$ creates problems for its implementation[3,48] and, to our best knowledge, even for atomic systems there were no reports on v_{xc} constructed with the integral formula (41).

Nevertheless, the procedure of Sec. III provides a reasonable accuracy, in particular, for the constructed function ϵ_{xc}. This function contains only the ''energetical'' components $\frac{1}{2}v_{\mathrm{xc}}^{\mathrm{hole}}$, $v_{c,\mathrm{kin}}$ of V_{xc} and it integrates to the energy E_{xc},

$$E_{\mathrm{xc}} = \int \rho(\mathbf{r})\epsilon_{\mathrm{xc}}^{\mathrm{CI}}(\mathbf{r})\,d\mathbf{r} = W_{\mathrm{xc}}^{\mathrm{CI}} + T^{\mathrm{CI}} - T_s \tag{42}$$

which, when obtained with a CI wave function of good quality, is a reasonable estimate of the accurate E_{xc} (see Sec. V for a discussion of the KS kinetic functionals). Furthermore, the dominating $\frac{1}{2}v_{\mathrm{xc}}^{\mathrm{hole}}(\mathbf{r})$ term of $\epsilon_{\mathrm{xc}}(\mathbf{r})$ is obtained directly from *ab initio* $\rho(\mathbf{r})$ and $\rho_2(\mathbf{r}_1,\mathbf{r}_2)$, providing also a reasonable local quality of ϵ_{xc} as a function of $\mathbf{r}$.

$v_{xc}(\mathbf{r})$ and $\epsilon_{xc}(\mathbf{r})$ constructed from the correlated $\rho(\mathbf{r},\mathbf{r}')$ and $\rho_2(\mathbf{r}_1,\mathbf{r}_2)$ contain important information about the local effect of the electron correlation and can serve as a reference for density functional approximations. In particular, this opens new possibilities for modeling of ϵ_{xc}, which became an essential part of the development of DFT.[1,2] When developing a new ϵ_{xc}, one can take into account not only the total E_{xc} values or the scaling and asymptotic properties of the E_{xc} functional, but also the local behavior of $\epsilon_{xc}(\mathbf{r})$ obtained from *ab initio* wave functions for a representative set of atomic and molecular systems. A promising option is to approximate directly the potential $\frac{1}{2}v_{xc}^{hole}(\mathbf{r})$ and kinetic $v_{c,kin}(\mathbf{r})$ components. Hopefully, an efficient approximation to v_{xc}^{hole} can be achieved with a function of the density ρ and its gradient, while $v_{c,kin}$, with its bond midpoint and intershell peaks may require a less traditional orbital-dependent approximation. The corresponding work, as well as the refinement of the procedure of $v_{xc}(\mathbf{r})$ and $\epsilon_{xc}(\mathbf{r})$ construction and its application to different types of bonding situations, is in progress.

ACKNOWLEDGMENTS

We gratefully acknowledge funding by the Netherlands Foundation for Scientific Research (NWO) and the Stichting Fundamenteel Onderzoek der Materie (FOM).

[1] R. M. Dreizler and E. K. U. Gross, *Density Functional Theory: An Approach to the Quantum Many-Body Problem* (Springer, Berlin, 1990).
[2] R. G. Parr and W. Yang, *Density Functional Theory of Atoms and Molecules* (Oxford University, New York, 1989).
[3] S. H. Werden and E. R. Davidson, in *Local Density Approximations in Quantum Chemistry and Solid State Physics* (Plenum, New York, 1982).
[4] C. O. Almbladh and A. C. Pedroza, Phys. Rev. A **29**, 2322 (1984).
[5] F. Aryasetiawan and M. J. Stott, Phys. Rev. B **38**, 2974 (1988).
[6] A. Nagy and N. H. March, Phys. Rev. A **39**, 5512 (1989).
[7] A. Görling and M. Ernzerhof, Phys. Rev. A **51**, 4501 (1995).
[8] Y. Wang and R. G. Parr, Phys. Rev. A **47**, 1591 (1993).
[9] R. van Leeuwen and E. J. Baerends, Phys. Rev. A **49**, 2421 (1994).
[10] Q. Zhao, R. C. Morrison, and R. G. Parr, Phys. Rev. A **50**, 2138 (1994).
[11] O. V. Gritsenko, R. van Leeuwen, and E. J. Baerends, Phys. Rev. A **52**, 1870 (1995).
[12] O. V. Gritsenko, R. van Leeuwen, and E. J. Baerends, J. Chem. Phys. **101**, 8955 (1994).
[13] J. D. Talman and W. F. Shadwick, Phys. Rev. A **14**, 36 (1976).
[14] K. Aashamar, T. M. Luke, and J. D. Talman, At. Data. Nucl. Data. Tables **22**, 443 (1978).
[15] J. D. Talman, Comput. Phys. Commun. **54**, 85 (1989).
[16] M. A. Buijse, E. J. Baerends, and J. G. Snijders, Phys. Rev. A **40**, 4190 (1989).
[17] P. Süle, O. V. Gritsenko, Á. Nagy, and E. J. Baerends, J. Chem. Phys. (to be published); **103**, 10085 (1995).
[18] G. Hunter, Int. J. Quantum Chem. **9**, 237 (1975).
[19] M. Levy and H. Ou-Yang, Phys. Rev. A **38**, 625 (1988).
[20] D. C. Langreth and J. P. Perdew, Solid State Commun. **17**, 1425 (1975).
[21] O. Gunnarsson and B. I. Lundqvist, Phys. Rev. B **13**, 4274 (1976).
[22] P. Hohenberg and W. Kohn, Phys. Rev. **136B**, 864 (1964).
[23] A. Savin, H. Stoll, and H. Preuss, Theor. Chim. Acta **70**, 407 (1986).
[24] V. R. Saunders and J. H. van Lenthe, Mol. Phys. **48**, 923 (1983).
[25] G. C. Lie and E. Clementi, J. Chem. Phys. **60**, 1275 (1974).
[26] M. A. Buijse, Ph.D. thesis, Vrije Universiteit, Amsterdam, The Netherlands, 1991.
[27] G. te Velde and E. J. Baerends, J. Comp. Phys. **99**, 84 (1992).
[28] O. V. Gritsenko, R. van Leeuwen, E. van Lenthe, and E. J. Baerends, Phys. Rev. A **51**, 1944 (1995).
[29] J. C. Slater, *Quantum Theory of Molecules and Solids* (McGraw–Hill, New York, 1974), Vol. 4.
[30] A. D. Becke, Phys. Rev. A **38**, 3098 (1988).
[31] S. H. Vosko, L. Wilk, and M. Nusair, Can. J. Phys. **58**, 1200 (1980).
[32] S. J. Chakravorty, S. R. Gwaltney, E. R. Davidson, F. A. Parpia, and C. Froese Fischer, Phys. Rev. A **47**, 3649 (1993).
[33] J. P. Perdew, R. G. Parr, M. Levy, and J. L. Balduz, Phys. Rev. Lett. **49**, 1691 (1982).
[34] U. von Barth, in *The Electronic Structure of Complex Systems*, NATO ASI Series B 113, edited by P. Phariseau and W. Temmerman (Plenum, New York, 1984).
[35] M. Levy, J. P. Perdew, and V. Sahni, Phys. Rev. A **30**, 2745 (1984).
[36] C. O. Almbladh and U. von Barth, Phys. Rev. B **31**, 3231 (1985).
[37] R. C. Morrison and Q. Zhao, Phys. Rev. A **51**, 1980 (1995).
[38] K. Ruedenberg, Rev. Mod. Phys. **39**, 326 (1962).
[39] M. J. Feinberg and K. Ruedenberg, J. Chem. Phys. **54**, 1495 (1971).
[40] A. Rozendaal and E. J. Baerends, Chem. Phys. **95**, 57 (1985).
[41] M. Levy and J. P. Perdew, Phys. Rev. A **32**, 2010 (1985).
[42] R. van Leeuwen, O. V. Gritsenko, and E. J. Baerends, Z. Phys. D **33**, 229 (1995).
[43] V. W. Maslen, Proc. Phys. Soc. (London) A **69**, 734 (1956).
[44] G. Sperber, Int. J. Quantum Chem. **6**, 881 (1972).
[45] W. L. Luken and D. N. Beratan, Theor. Chim. Acta **61**, 265 (1982).
[46] M. A. Buijse and E. J. Baerends, in *Density Functional Theory of Molecules, Clusters and Solids*, edited by D. E. Ellis (Kluwer, Amsterdam, 1995), p. 1.
[47] J. B. Krieger, Y. Li, and G. J. Iafrate, Phys. Rev. A **45**, 101 (1992).
[48] A. Görling, Phys. Rev. A **46**, 3753 (1992).